

LARGE AMOUNTS OF OPTICALLY OBSCURED STAR FORMATION IN THE HOST GALAXIES OF SOME TYPE 2 QUASARS

M. LACY,¹ A. SAJINA,¹ A. O. PETRIC,^{1,2} N. SEYMOUR,¹ G. CANALIZO,³ S. E. RIDGWAY,⁴
 L. ARMUS,¹ AND L. J. STORRIE-LOMBARDI¹

Received 2007 August 1; accepted 2007 September 21; published 2007 October 12

ABSTRACT

We present *Hubble Space Telescope* images and spectral energy distributions from optical to infrared wavelengths for a sample of six $0.3 < z < 0.8$ type 2 quasars selected in the mid-infrared using data from the *Spitzer Space Telescope*. All the host galaxies show some signs of disturbance. Most seem to possess dusty, star-forming disks. The disk inclination, estimated from the axial ratio of the hosts, correlates with the depth of the silicate feature in the mid-infrared spectra, implying that at least some of the reddening toward the AGN arises in the host galaxy. The star formation rates in these objects, as inferred from the strengths of the PAH features and far-infrared continuum, range from 3 to $90 M_{\odot} \text{ yr}^{-1}$, but are mostly much larger than those inferred from the [O II] $\lambda 3727$ emission-line luminosity, due to obscuration. Taken together with studies of type 2 quasar hosts from samples selected in the optical and X-ray, this is consistent with previous suggestions that two types of extinction processes operate within the type 2 quasar population, namely, a component due to the dusty torus in the immediate environment of the AGN, and a more extended component due to a dusty, star-forming disk.

Subject headings: galaxies: Seyfert — galaxies: starburst — infrared: galaxies — quasars: general

1. INTRODUCTION

Coevolution of black holes and their host galaxies is a prediction of most models for the observed close correlation between black hole mass and bulge luminosity/velocity dispersion in local galaxies (e.g., Kauffmann & Haehnelt 2000; di Matteo et al. 2005). Studies of local active galactic nuclei (AGNs) and type 1 (unobscured) quasars show a correlation between AGN luminosity in the mid-infrared and starburst luminosity, estimated from the far-infrared emission and/or polycyclic aromatic hydrocarbon (PAH) features (Schweitzer et al. 2006; Shi et al. 2006; Maiolino et al. 2007), and the host galaxies of quasars with strong far-infrared excesses do seem to be forming stars (Canalizo & Stockton 2001). However, in general, host galaxy imaging studies in the optical and near-IR do not suggest that strong star formation occurs simultaneously with quasar activity in the majority of quasars. Imaging of type 1 quasar host galaxies show that the hosts of luminous quasars tend to be elliptical galaxies with little obvious signs of disturbance in *Hubble Space Telescope* (*HST*) images (e.g., Floyd et al. 2004), and only about 30% of quasars show signs of mergers or interactions in *HST* or adaptive optics images (Marble et al. 2003; Guyon et al. 2007), although deeper (several orbit) *HST* ACS imaging often reveals faint tidal features in quasar hosts (Canalizo et al. 2007; N. Bennert et al. 2007, in preparation). Studies of type 2 (obscured) quasars have so far been consistent with this picture, and with the idea that the obscuration takes place in a nuclear torus. Sturm et al. (2006), in their *Spitzer* study of X-ray-selected type 2 quasars, make the claim that “type 2 quasars are not ULIRGs” based on featureless mid-infrared spectra. *HST* imaging studies of the host galaxies of type 2 quasars selected from the Sloan Digital Sky Survey (SDSS) show that they are consistent with being hosted by rel-

atively undisturbed elliptical galaxies, once the likely effects of scattered light are accounted for (Zakamska et al. 2006).

In this Letter, we present results of *Spitzer* spectroscopy and photometry and *HST* imaging of a sample of type 2 quasars, and we discuss the implications for the coevolution of galaxies and black holes. Our sample is selected in the mid-infrared, which is less sensitive to reddening in the host galaxy than X-ray or optical selection, and their type 2 nature allows us to image the central regions of the host with high fidelity. The combination of infrared spectral energy distributions (SEDs) and optical imaging of this sample thus allows us for the first time to present a coherent picture of the nature of the star formation in the host galaxies of type 2 quasars.

2. OBSERVATIONS

We selected all six candidate type 2 quasars with $0.3 < z < 0.8$ from the 1 mJy $8 \mu\text{m}$ flux density-limited sample of Lacy et al. (2004). The redshift range ensures that these objects are luminous enough to be on or above the quasar/Seyfert divide in the mid-infrared ($5 \mu\text{m}$ luminosity, $L_{5\mu\text{m}} \sim 10^{23.6} \text{ W Hz}^{-1}$; Lacy et al. 2005a) but low enough for rest-frame *B* band to be within the F814W filter of the Advanced Camera for Surveys (ACS) aboard *HST*. The objects were observed with the Multiband Imaging Photometer (MIPS) and Infrared Spectrograph (IRS) as part of *Spitzer* program 20083, and with *HST* as program GO-10848 (Table 1). Redshifts were obtained and optical spectral classifications attempted (Lacy et al. 2007). Low-dispersion spectra were also obtained with the Spex instrument (Rayner et al. 2003) in prism mode at the Infrared Telescope Facility (IRTF).

The IRS data were obtained in stare mode, using the short-low and long-low modules. The IRS short-low data had a background image subtracted, made by taking a median of all the short-low observations in the Astronomical Observation Request. The long-low data were combined by subtracting nodded pairs, then combining the pairs with minmax rejection. Extraction was performed using the SPICE tool,⁵ with optimal

¹ Spitzer Science Center, Caltech, Mail Code 220-6, Pasadena, CA 91125; mlacy@ipac.caltech.edu, sajina@ipac.caltech.edu, lisa@ipac.caltech.edu.

² Columbia University, New York, NY 10027; andreea@ipac.caltech.edu.

³ University of California, Riverside, CA 92521; gabriela.canalizo@ucr.edu.

⁴ NOAO, Colina El Pino s/n, Casilla 603, La Serena, Chile; seridgway@ctio.noao.edu.

⁵ See <http://ssc.spitzer.caltech.edu/postbcd/spice.html>.

TABLE 1
OBSERVATIONS

Name	IRS reqkey	MIPS reqkey	ACS Filters
SSTXFLS J172123.1+601214	14016768	14018304	F625W, F435W
SSTXFLS J171147.4+585839	14016000	14017536	F814W, F555W
SSTXFLS J171324.2+585549	14016256	14017792	F775W, F475W
SSTXFLS J171831.5+595317	14016512	14018048	F775W, F475W
SSTXFLS J171106.8+590436	14015744	14017280	F775W, F475W
SSTXFLS J172458.3+591545	14017024	14018560	F775W, F475W

extraction. Aperture photometry was performed on the pipeline (post-BCD) MIPS mosaics using standard aperture corrections.⁶

The ACS data were taken in two filters, one longward and one shortward of the 4000 Å break in the rest frame of the galaxy. Observations consisted of four exposures in each filter in a standard dither pattern, for one orbit per object per filter. The ACS pipeline mosaics were also adequate for the analysis performed here. A full analysis of the data will be presented in N. Seymour et al. (2007, in preparation).

Four of our six objects were easily classified as type 2 quasars in Lacy et al. (2007) based on well-established optical emission-line diagnostics. However, SSTXFLS J171106.8+590436 and SSTXFLS J172458.3+591525 had optical emission-line properties that were ambiguous. For SSTXFLS J172458.3+591525, we are able to estimate a $([\text{S II}] \lambda\lambda 6719+6732)/(\text{H}\alpha + [\text{N II}])$ ratio of 0.4 from the IRTF/Spex spectrum, which, together with an $[\text{O III}]/\text{H}\beta$ ratio of 10 and assuming typical $[\text{N II}]/\text{H}\alpha$ ratios of 0.1–1.6, places this object firmly among the AGNs in the diagnostic plot of Kewley et al. (2006), with a range in $\log([\text{S II}]/\text{H}\alpha) \approx -0.4$ to 0.1. In the case of SSTXFLS J171106.8+590436, the $\text{H}\alpha$ and $[\text{S II}]$ lines are too weak to do this. However, the very high $[\text{O III}]/\text{H}\beta$ ratio of $>10:1$, detection of $\text{He II} \lambda 6686$, and a marginal detection of $[\text{Ne V}] \lambda 4.3 \mu\text{m}$ in the IRS spectrum make it very likely that an AGN classification for the optical spectrum is correct. We thus assume for the rest of this Letter that all six objects contain powerful AGNs.

3. ANALYSIS

We fit our SEDs and spectra using a model based on those of Sajina et al. (2005, 2006). The IRS spectra were fit directly, along with photometric points in r , i , and z bands from the SDSS, IRAC 3.6, and $4.5 \mu\text{m}$ data (Lacy et al. 2005b), MIPS 70 and $160 \mu\text{m}$ data (Frayser et al. 2006 and this Letter), and near-infrared photometry from IRTF. We also checked the IRS spectrophotometry against the IRAC 5.8 and $8.0 \mu\text{m}$ and MIPS 24 μm (Fadda et al. 2006) broadband photometry, and found them to agree within $\approx 10\%$.

The far-infrared (FIR) emission was fit as a modified blackbody with temperature $\approx 45 \text{ K}$. A warm (small grain) component was included with a power-law index of ≈ 2 and cutoffs at high

and low frequency. The FIR luminosity, L_{FIR} , was estimated by summing the warm and cold components. The hot dust component was based on a power law with variable spectral index. The long-wavelength cutoff was determined by a fit of a Fermi function to the least star-forming AGNs in our sample, SSTXFLS J172123.1+601214, which shows a turn-down in the hot dust emission beginning at a rest-frame wavelength $\approx 20 \mu\text{m}$.

Netzer et al. (2007) also suggest that the AGN-related hot dust emission starts to decrease beyond $\approx 20 \mu\text{m}$ in type 1 quasars. The hot dust emission was exponentially cut off at high frequencies with a variable cutoff frequency. The unreddened luminosity of the AGN, L_{AGN} , was estimated by integrating this component. The hot dust component is then reddened by the Galactic center extinction law of Chiar & Tielens (2006), likely to be a good approximation to the extreme density environments of AGNs (Sajina et al. 2007).

A modified version of the starburst PAH emission template of Sajina et al. (2007) was used to fit the PAH features. AGNs are known to modify the PAH spectra (Smith et al. 2007). In particular, for our objects, we found a better match by boosting the $7.7 \mu\text{m}$ feature in the template by hand. This PAH template was fitted to the SEDs of all galaxies except SSTXFLS J172123.1+601214, which had a small amount of silicate emission added instead. Total PAH luminosities, L_{PAH} , were determined by integrating over the fitted template. Finally, a 5 Gyr old single stellar population from Bruzual & Charlot (2003) was fit to the optical points. The basic properties of the fits are listed in Table 2.

Parameters that are not well constrained by the data (e.g., the warm dust continuum strength in objects not detected at $160 \mu\text{m}$) are held fixed. Full details of the fitting process will be given in a future paper (S. Ridgway et al. 2007, in preparation).

4. DISCUSSION

We first address the amount of star formation in the host galaxies. Star formation rates (SFRs) derived from FIR emission alone are suspect for quasars, as reprocessed quasar emission can, in principle, contribute to the FIR flux. In the five of six cases in which PAHs are detected, however, they show typical ratios of PAH/FIR luminosities over a wide range of L_{FIR} (0.02–0.06 in total PAH integrated over our template, corresponding to 0.0014–0.0042 in the $6.2 \mu\text{m}$ feature, within

TABLE 2
HOST GALAXY PROPERTIES

Object	z	$\log(L_{\text{AGN}})$ (L_{\odot})	$\log(L_{\text{FIR}})$ (L_{\odot})	$\log(L_{\text{PAH}})$ (L_{\odot})	$\log(L_{[\text{O III}]})$ (L_{\odot})	S_{sil}	Axial Ratio	SFR (FIR) ($M_{\odot}\text{yr}^{-1}$)	SFR ([O II]) ^a ($M_{\odot}\text{yr}^{-1}$)
SSTXFLS J172123.1+601214	0.325	11.4	10.6	<9.4	8.17	...	0.63 ± 0.02	3.3	3.9
SSTXFLS J171147.4+585839	0.800	12.1	11.7	10.5	8.44	-0.21	0.96 ± 0.02	56	7.2
SSTXFLS J171324.2+585549	0.609	11.8	11.3	9.8	8.26	-0.34	0.79 ± 0.01	16	4.8
SSTXFLS J171831.5+595317	0.700	11.9	12.0	10.3	8.45	-0.53	0.76 ± 0.05	87	7.4
SSTXFLS J171106.8+590436	0.462	11.8	11.5	10.1	7.49	-1.56	0.67 ± 0.01	33	0.8
SSTXFLS J172458.3+591545	0.494	11.6	11.6	10.4	7.91	-1.97	0.24 ± 0.02	37	2.1

^a From Kewley et al. (2004), assuming solar metallicity.

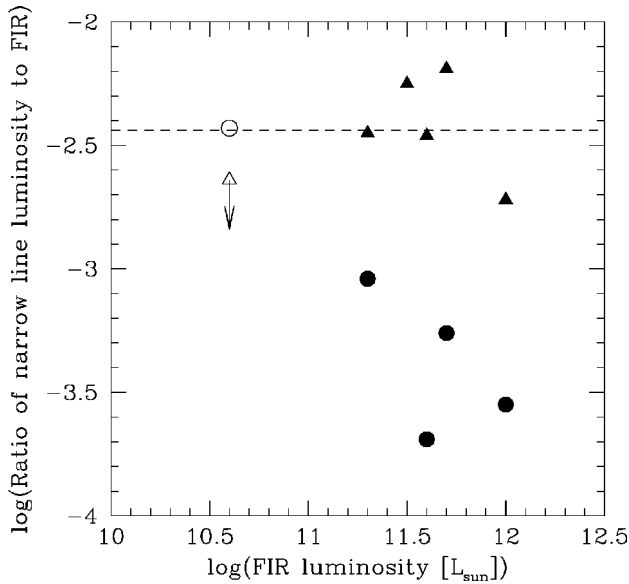


FIG. 1.—Ratio of narrow-line luminosity in [O II] $\lambda 3727$ to FIR luminosity (circles) and in [Ne II] $12.8 \mu\text{m}$ to FIR luminosity (triangles). Host galaxies dominated by a disk component are shown as filled symbols. SSTXFLS J172123.1+601214, which has an elliptical host, is shown with open symbols. The dashed line is the ratio of [O II] to FIR luminosity expected in an unextincted starburst.

the range for star-forming galaxies and ULIRGs seen by Peeters et al. [2004] of $\sim 0.005\text{--}0.1$). This indicates that the bulk of the FIR emission is indeed likely to be from star formation (see also A. Sajina et al. 2007, in preparation). A similar result has been found for type 1 quasars by Schweitzer et al. (2006). As Figure 1 shows, however, the [O II] $\lambda 3727$ emission (from the spectra of Lacy et al. [2007], aperture-corrected using the SDSS photometry) is significantly below that expected in an unreddened starburst in most cases, particularly for the objects with high-FIR luminosities. This is consistent with the result of Ho (2005), who found low [O II] $\lambda 3727$ emission from type 1 quasar hosts compared to their expected SFRs based on measurements of molecular gas. However, the ratio of the [Ne II] $12.8 \mu\text{m}$ to the FIR luminosity is similar for all our objects. [Ne II] is of similar ionization to [O II] and is also therefore dominated by emission from the starburst. This suggests that dust reddening is to blame for the lack of [O II] $\lambda 3727$ emission and is also consistent with the host galaxy colors and morphologies. As can be seen in Figure 2, the host galaxies of the objects with high L_{FIR} are typically disturbed, red objects, likely to be late-stage merger remnants. This suggests that star formation in a significant fraction of quasar host galaxies is heavily obscured in the optical.

Obscuration by dusty star-forming regions also seems to affect the extinction to the AGN. Figure 3 shows a plot of axial ratio of the host galaxy (measured using the *ellipse* task in IRAF on the longer wavelength image) versus the depth of the

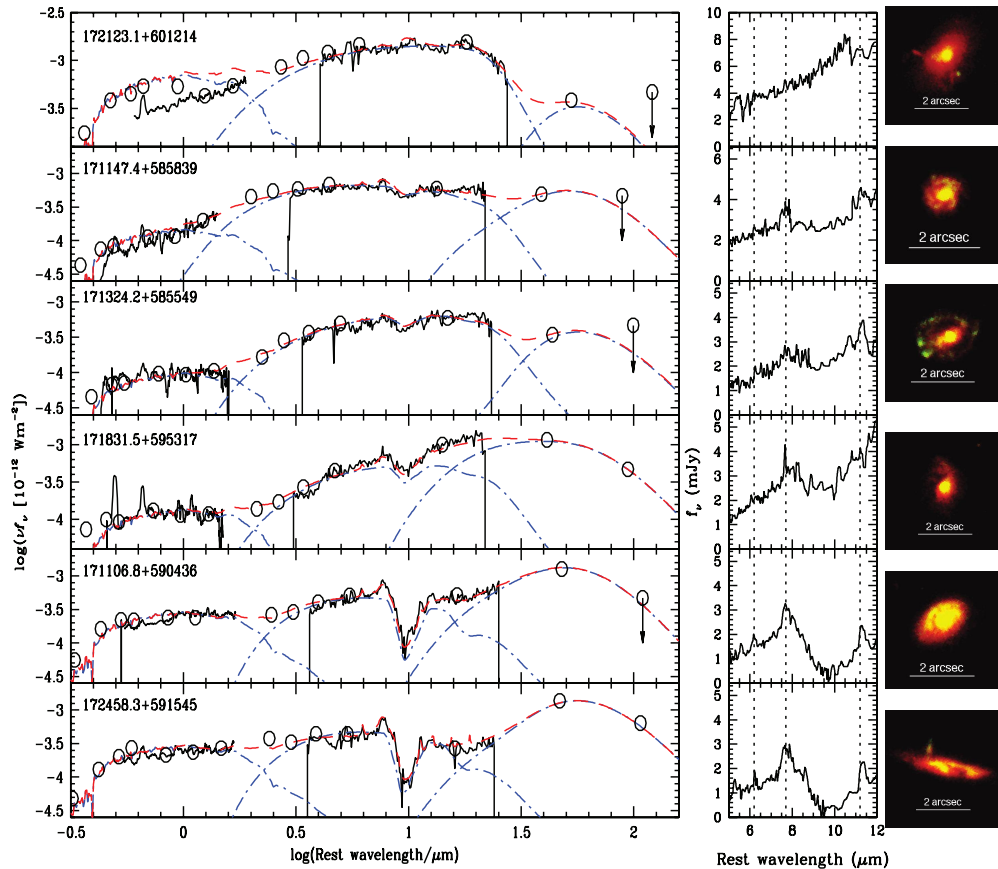


FIG. 2.—SEDs and *HST* images of the six type 1 quasars, in order of increasing silicate absorption. The solid black lines are the IRTF Spex and *Spitzer* IRS spectra (both smoothed to reduce noise) and the black open circles photometry from SDSS, IRTF, and *Spitzer*. The model fit is shown as the red dashed line, with (from left to right) the stellar component, hot dust component (including absorption, but excluding PAH emission), and sum of warm and cold dust components shown as blue dash-dotted lines. To the right of the SEDs we show expanded plots of the IRS spectra around the PAH wavelengths. The ACS images have the long-wavelength image colored red, and the short-wavelength image in green.

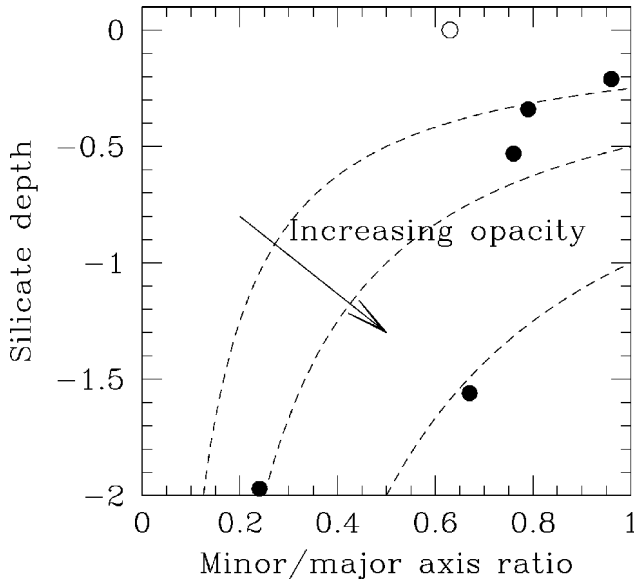


FIG. 3.—Absorption depth in the $9.7\ \mu\text{m}$ silicate feature plotted against axial ratio. Symbols are the same as in Fig. 2. The dashed lines represent the predictions of simple uniform disk models of differing opacity measured perpendicular to the disk.

$9.7\ \mu\text{m}$ silicate feature, S_{sil} , as defined by Levenson et al. (2006). Although our sample is small, the five of our six host galaxies with apparent or possible disklike structures, and profiles close to exponential disks (excluding morphological disturbances and bulge components), represented by the solid points, seem to show a trend in the sense that the more highly extincted objects have more edge-on inclinations (lower axial ratios). The one galaxy that does not appear disklike, SSTXFLS J172123.1+601214 (*open symbol*), has an underlying $r^{1/4}$ law profile and is probably an example of an elliptical host merging with a smaller gas-rich galaxy and lacks the large amount of star formation seen in the mergers of two gas-rich galaxies. In this case, the obscuration is probably almost entirely due to the torus. For the disklike hosts, a simple uniform dusty disk model appears to work for most, with a spread of about a factor of 2 in opacity for a line of sight perpendicular to the disk. One object (SSTXLFS J171106.8+590436), however, would have a high opacity in

this model even if viewed face-on, corresponding to $S_{\text{sil}} \approx -1$. This may be because the extinction is patchy, and a high inclination significantly increases the chance of the line of sight passing through a high-opacity region such as a dense molecular cloud. Our two most obscured type 2 quasars (with $S_{\text{sil}} = -1.6$ and -2) have silicate absorption as deep or deeper than the most obscured AGNs in the sample of Shi et al. (2006). These radio galaxies and Seyfert 2s have $S_{\text{sil}} \geq -1.6$, suggesting that extinction can be very extreme in the radio-quiet quasar population.

The implication of our result is that many type 2 quasars have at least a component of the extinction toward the nucleus from an extended, star-forming disk on scales of kiloparsecs, in addition to, or instead of, the traditional obscuring torus, which interferometry suggests is only a few parsecs in size (Jaffe et al. 2004). Previous suggestions that the host galaxy can contribute significantly to the AGN extinction in type 2 objects have been made by Martínez-Sansigre et al. (2006) and Rigby et al. (2006), based on optical emission-line properties. Our results suggest that a significant fraction of the quasar population have their AGNs obscured by star-forming regions in their host galaxies. Thus, studying obscured quasars is essential if we are to understand the origin of the links between the evolution of quasars and their hosts.

We thank the referee for a helpful report. M. L. and A. O. P. were visiting astronomers at the IRTF, which is operated by the University of Hawaii under Cooperative Agreement NCC 5-538 with the National Aeronautics and Space Administration (NASA), Science Mission Directorate, Planetary Astronomy Program. This work is based on observations made with the *Spitzer Space Telescope*, which is operated by the Jet Propulsion Laboratory, California Institute of Technology, under a contract with NASA. Support for this work was provided by NASA through an award issued by JPL/Caltech. This work is also based on observations made with the NASA/ESA *Hubble Space Telescope*, obtained at the Space Telescope Science Institute (STScI), operated by the Association of Universities for Research in Astronomy, Inc., under NASA contract NAS 5-26555, and are associated with program 10848, partly supported by a grant from STScI.

REFERENCES

- Bruzual, G., & Charlot, S. 2003, MNRAS, 344, 1000
 Canalizo, G., Bennert, N., Jungwiert, B., Stockton, A., Schweizer, F., Lacy, M., & Peng, C. 2007, ApJ, 669, in press
 Canalizo, G., & Stockton, A. N. 2001, ApJ, 555, 719
 Chiar, J. E., & Tielens, A. G. G. M. 2006, ApJ, 637, 774
 di Matteo, T., Springel, V., & Hernquist, L. 2005, Nature, 433, 604
 Fadda, D., et al. 2006, AJ, 131, 2859
 Floyd, D., Kukula, M. J., Dunlop, J. S., McLure, R. J., Miller, L., Percival, W. J., Baum, S. A., O'Dea, C. P. 2004, MNRAS, 355, 196
 Frayer, D. T., et al. 2006, AJ, 131, 250
 Guyon, O., Sanders, D. B., & Stockton, A. 2006, ApJS, 166, 89
 Ho, L. 2005, ApJ, 629, 680
 Jaffe, W., et al. 2004, Nature, 429, 47
 Kauffmann, G., & Haehnelt, M. G. 2000, MNRAS, 311, 576
 Kewley, L. J., Geller, M. J., & Jansen, R. A. 2004, AJ, 127, 2002
 Kewley, L. J., Groves, B., Kauffmann, G., & Heckman, T. 2006, MNRAS, 372, 961
 Lacy, M., Petric, A. O., Sajina, A., Canalizo, G., Storrie-Lombardi, L. J., Armus, L., Fadda, D., & Marleau, F. R. 2007, AJ, 133, 186
 Lacy, M., et al. 2004, ApJS, 154, 166
 ———. 2005a, Mem. Soc. Astron. Italiana, 76, 154
 ———. 2005b, ApJS, 161, 41
 Levenson, N. A., Sirocky, M. M., Hao, L., Spoon, H. H. W., Marshall, J. A., Elitzur, M., & Houck, J. R. 2007, ApJ, 654, L45
 Maiolino, R., Shemmer, O., Imanishi, M., Netzer, H., Oliva, E., Lutz, D., & Sturm, E. 2007, A&A, 468, 979
 Marble, A. R., Hines, D. C., Schmidt, G. D., Smith, P. S., Surace, J. A., Armus, L., Cutri, R. M., & Nelson, B. O. 2003, ApJ, 590, 707
 Martínez-Sansigre, A., et al. 2006, MNRAS, 370, 1479
 Netzer, H., et al. 2007, ApJ, 666, 806
 Peeters, E., Spoon, H. W. W., & Tielens, A. G. G. M. 2004, ApJ, 613, 986
 Rayner, J. T., et al. 2003, PASP, 115, 362
 Rigby, J. R., Rieke, G. H., Donley, J. L., Alonso-Herrero, A., & Perez-González, P. G. 2006, ApJ, 645, 115
 Sajina, A., Lacy, M., & Scott, D. 2005, ApJ, 621, 256
 Sajina, A., Scott, D., Dennefeld, M., Dole, H., Lacy, M., & Lagache, G. 2006, MNRAS, 369, 939
 Sajina, A., Yan, L., Armus, L., Choi, P., Fadda, D., Helou, G., & Spoon, H. 2007, ApJ, 664, 713
 Schweitzer, M., et al. 2006, ApJ, 649, 79
 Shi, Y., et al. 2006, ApJ, 653, 127
 Smith, J. D. T., et al. 2007, ApJ, 656, 770
 Sturm, E., Hasinger, G., Lehmann, I., Mainieri, V., Genzel, R., Lehnert, M. D., Lutz, D., & Tacconi, L. J. 2006, ApJ, 642, 81
 Zakamska, N. L., et al. 2006, AJ, 132, 1496